BJ www.biochemj.org

BJ Cell

Biochem. J. (2012) **444**, 89–96 (Printed in Great Britain) doi:10.1042/BJ20120209

online data

89

Coronin 1C harbours a second actin-binding site that confers co-operative binding to F-actin

Keefe T. CHAN*†, David W. ROADCAP*, Nicholas HOLOWECKYJ* and James E. BEAR*†[1]

*Lineberger Comprehensive Cancer Center and Department of Cellular and Developmental Biology, University of North Carolina at Chapel Hill, NC 27599, U.S.A., and †Howard Hughes Medical Institute, University of North Carolina at Chapel Hill, NC 27599, U.S.A.

Dynamic rearrangement of actin filament networks is critical for cell motility, phagocytosis and endocytosis. Coronins facilitate these processes, in part, by their ability to bind F-actin (filamentous actin). We previously identified a conserved surface-exposed arginine (Arg^{30}) in the β-propeller of Coronin 1B required for F-actin binding *in vitro* and *in vivo*. However, whether this finding translates to other coronins has not been well defined. Using quantitative actin-binding assays, we show that mutating the equivalent residue abolishes F-actin binding in Coronin 1A, but not Coronin 1C. By mutagenesis and biochemical competition, we have identified a second actin-binding site in the unique region of Coronin 1C. Interestingly, leading-edge localization of Coronin 1C in fibroblasts requires the conserved site in the β-propeller, but not the site in the unique region. Furthermore, in contrast with Coronin 1A and Coronin 1B, Coronin 1C displays highly co-operative binding to actin filaments. In the present study, we highlight a novel mode of coronin regulation, which has implications for how coronins orchestrate cytoskeletal dynamics.

Key words: actin, co-operative binding, coronin, lamellipodia.

INTRODUCTION

Coronins, a family of highly conserved actin-binding proteins originally identified in *Dictyostelium* [1], have emerged as key regulators of actin dynamics via effects on assembly by the Arp2/3 (actin-related protein 2/3) complex and disassembly by cofilin [2]. Mammalian genomes contain at least six coronin genes organized into three classifications [3]. Most functional studies have focused on Coro1s (Type I coronins) (Coro1A, Coro1B and Coro1C). Coro1B and Coro1C are ubiquitously expressed isoforms, whereas Coro1A has a primarily haematopoietic expression pattern. Genetic deletion of Coro1A in mice results in severe defects in T-lymphocyte trafficking and chemotaxis [4]. Coro1B localizes to the leading edge of migrating fibroblasts [5] and its depletion alters lamellipodial architecture and whole-cell motility [6]. Like Coro1B, Coro1C localizes to lamellipodia and interacts with the Arp2/3 complex [7–9]; however, Coro1C may have additional roles in membrane trafficking [10] and tumour metastasis [11].

The crystal structure of Coro1A revealed that the most prominent structural characteristic is a seven-bladed WD40 repeat-containing β-propeller [12]. The β-propeller, a scaffold for protein–protein interactions [13], is flanked by N- and C-terminal extensions that contribute to its stability, followed by a highly variable unique region and a coiled-coil domain. Although the structure of the unique region has not been resolved, it has been shown to participate in coronin function. Yeast coronin Crn1p was initially identified as a microtubule-binding protein via the unique region [14]. In addition, a CA-like sequence, conserved in WASP (Wiskott–Aldrich syndrome protein)/SCAR (suppressor of cAMP receptor) proteins, is present in the unique region of yeast coronin and regulates the activity of the Arp2/3 complex [15]. The primary role of the coiled-coil domain is in coronin oligomerization [12,16,17].

Coronins were first identified by their ability to bind to F-actin (filamentous actin), but their actin-binding function is incompletely understood. Early studies attempted to address this by using truncation mutants [9,18–21]. The resolution of the crystal structure of Coro1A [12] suggested that the resulting proteins from truncations or deletions of portions of the β-propeller are likely to adopt unstable conformations. We provided the first direct demonstration that F-actin binding is essential for coronin function *in vitro* and *in vivo* by identifying a conserved arginine residue (Arg^{30}) on the surface of the β-propeller in Coro1B, which when mutated abolished F-actin binding [22]. Three-dimensional reconstructions further validated the requirement of the conserved site in the β-propeller and have also identified potential non-contiguous surfaces for the Coro1A–actin interaction [23]. A recent report on yeast coronin showed similar results that mutations in residues in a ridge extending across the side of the β-propeller disrupted F-actin binding [24]. Yeast coronin may contain a second lower-affinity actin-binding site in the coiled-coil domain that inhibits cofilin activity, but this site has not been mapped at high resolution [25]. However, another study has found no detectable actin binding for a fragment containing the coiled-coil domain [15].

In the present paper, we sought to provide further characterization of the actin-binding function of the mammalian Coro1s. In our analysis, we not only confirm our previous observations concerning the role of Arg^{30} in actin binding, but also reveal the unexpected findings that one member, Coro1C, contains a second actin-binding site and binds co-operatively to actin filaments.

EXPERIMENTAL

Cell culture and viral transduction

HEK (human embryonic kidney)-293FT cells (Invitrogen) were used to generate recombinant protein. IA32 (Ink/Arf-null) mouse embryonic fibroblasts were cultured as described previously [26]. Lentivirus production and infection were performed as described previously [27].

Abbreviations used: Arp2/3, actin-related protein 2/3; Coro1, Type I coronin; F-actin, filamentous actin; GFP, green fluorescent protein; IA32, Ink/Arf-null; NS, non-targeting; shRNA, short hairpin RNA.

[1] To whom correspondence should be addressed (email jbear@email.unc.edu).

Anti-Coro1C antibody production

An antibody against Coro1C was generated using an immunogen containing the human C-terminus (unique region and coiled-coil) by the University of North Carolina Monoclonal Antibody Core, collected and concentrated. Anti-Coro1C antibody (clone 22.51.1.10) was used for immunoblotting experiments.

Molecular cloning

Coro1C mutations were generated by overlap extension PCR and inserted into the multiple cloning site of the pTT5SH8Q2 vector that contains the StrepTagII and His_8 affinity tags.

The shRNA (short hairpin RNA) targeting mouse Coro1C was designed according to the instructions found at http://en.dogeno.us/2shrna/ and cloned into the HpaI/XhoI sites of pLL5.0(GFP) using methods described previously [6]. The 19-nt target sequence for mouse Coro1C is GACGGGACGAATTGACAAA. Wild-type and mutant versions of human Coro1C, which were not targeted by mouse Coro1C shRNA, were cloned into the multi-cloning site of pLL5.0(GFP). The NS (non-targeting) shRNA was described previously [6].

Expression and purification of recombinant coronin protein

Recombinant coronin protein was expressed and purified from a mammalian expression system as described previously [6].

Actin cosedimentation

Human platelet actin (Cytoskeleton) was depolymerized in general actin buffer [5 mM Tris/HCl (pH 8.0) and 0.2 mM $CaCl_2$] for 1 h at room temperature (23 °C) and pre-cleared by ultracentrifugation at 23 psi (100000 ***g*** for 15 min at 25 °C with an A-100/18 rotor; 1 psi = 6.9 kPa) in a Beckman Airfuge. Actin was polymerized by adding 1/10 vol. of polymerization buffer (500 mM KCl, 20 mM $MgCl_2$ and 10 mM ATP) and incubating at room temperature for 1 h.

Recombinant coronin proteins were incubated with actin at room temperature for 1 h and sedimented at 100000 ***g*** for 30 min. Pellets and supernatants were run on SDS/PAGE gels and analysed by Coomassie Blue staining or immunoblotting. Coomassie Blue-stained gels were scanned using an Odyssey Infrared Imager (LI-COR Biosciences) and images were despeckled using ImageJ (http://rsbweb.nih.gov/ij/).

To determine the binding affinity of coronin to F-actin, we used an established supernatant depletion method [22,28]. Coronin bound to F-actin was determined indirectly by immunoblotting the supernatant and quantified by densitometry. Binding curves were fitted to the experimental data with Graphpad Prism software.

Immunofluorescence and image analysis

For immunofluorescent cell staining, cells were fixed, stained and mounted as described previously [29]. Cells were stained with an anti-cortactin antibody (1:400 dilution; Millipore) and Alexa Fluor® 647-phalloidin (1:500 dilution; Molecular Probes). Cells were imaged using an Olympus FV1000 confocal microscope equipped with a 40× (1.3 numerical aperture) oil-immersion objective. A maximum intensity projection was generated from a *z*-stack (7 slices, 1.28 μm/slice). To plot the distribution of a protein around the cell edge, a previously published contour-based ImageJ macro was used [6]. Briefly, the images from GFP (green fluorescent protein) fluorescence, cortactin and phalloidin staining were merged into a single image, which was converted to a binary mask by thresholding the cell based on the actin image. A hand-drawn polygon mask was used to exclude those regions lacking peripheral cortactin staining. Dilation or erosion operations were iteratively performed to create a series of contour lines both inside and outside the perimeter of the cell (http://www.unc.edu/~cail/code/edge2.txt). Pixel intensities from -6 μm to 0 μm were extracted from each channel and plotted as a function of distance from the edge of the cell. Extracted pixel intensities were exported to Excel for analysis and Prism (GraphPad) for graphing.

RESULTS

Mutation in a conserved arginine residue blocks F-actin binding in Coro1A and Coro1B, but not Coro1C

We previously identified a conserved arginine residue (Arg^{30}) within the β-propeller domain of Coro1B, which when mutated to aspartate (R30D) abolished F-actin binding [22]. This residue is present in other Coro1s (Figure 1A) and subsequent studies have confirmed the requirement for the equivalent residue in Coro1A [30,31], but this has not been directly tested for Coro1C. In order to address this, we utilized a mammalian expression system to produce recombinant wild-type and mutant coronin proteins with >99 % purity (Supplementary Figure S1 at http://www.BiochemJ.org/bj/444/bj4440089add.htm). As expected, co-sedimentation assays demonstrated that all Coro1s sediment efficiently with F-actin (Figure 1B). Conversely, the arginine-to-aspartic acid mutations in Coro1A and Coro1B abolished F-actin binding. To our surprise, the R28D mutation in Coro1C failed to block F-actin binding. We verified further that this effect was not due to Coro1C sedimenting independently of its ability to bind F-actin (Supplementary Figure S2 at http://www.BiochemJ.org/bj/444/bj4440089add.htm).

If Coro1s share a common binding site through the β-propeller, we postulated that they should compete for binding to F-actin. The primary sequence of Coro1B is longer than Coro1C and Coro1A by 10 and 23 amino acids respectively; however, Coro1B migrates approximately 10 kDa slower on SDS/PAGE gels. This property allowed us to distinguish between Coro1A and Coro1C from Coro1B and perform biochemical competition experiments. We performed cosedimentation assays under equilibrium conditions to test for competition. Coro1B was able to compete with Coro1A (Figure 1C), and conversely Coro1A was able to compete with Coro1B (Figure 1D). Increasing concentrations of Coro1C also effectively competed with Coro1B (Figure 1E). In contrast, increasing concentrations of Coro1B (within the concentration range tested) were unable to compete with Coro1C for binding to F-actin (Figure 1F). These data indicate that Coro1A and Coro1B bind F-actin through a synonymous site on the β-propeller. However, the failure of the R28D mutation on Coro1C to block actin binding and the inability of Coro1B to effectively compete with Coro1C for actin binding raise the intriguing possibility that Coro1C may harbour an additional actin-binding site.

Coro1C harbours an additional actin-binding site within the unique region

A previous study using truncation mutants of Coro1C suggested that an actin-binding site might reside within the unique region of the protein [9]; however, this site has not been clearly defined. We compared the sequences of the unique regions between the Coro1s and noted a patch of charged residues within the

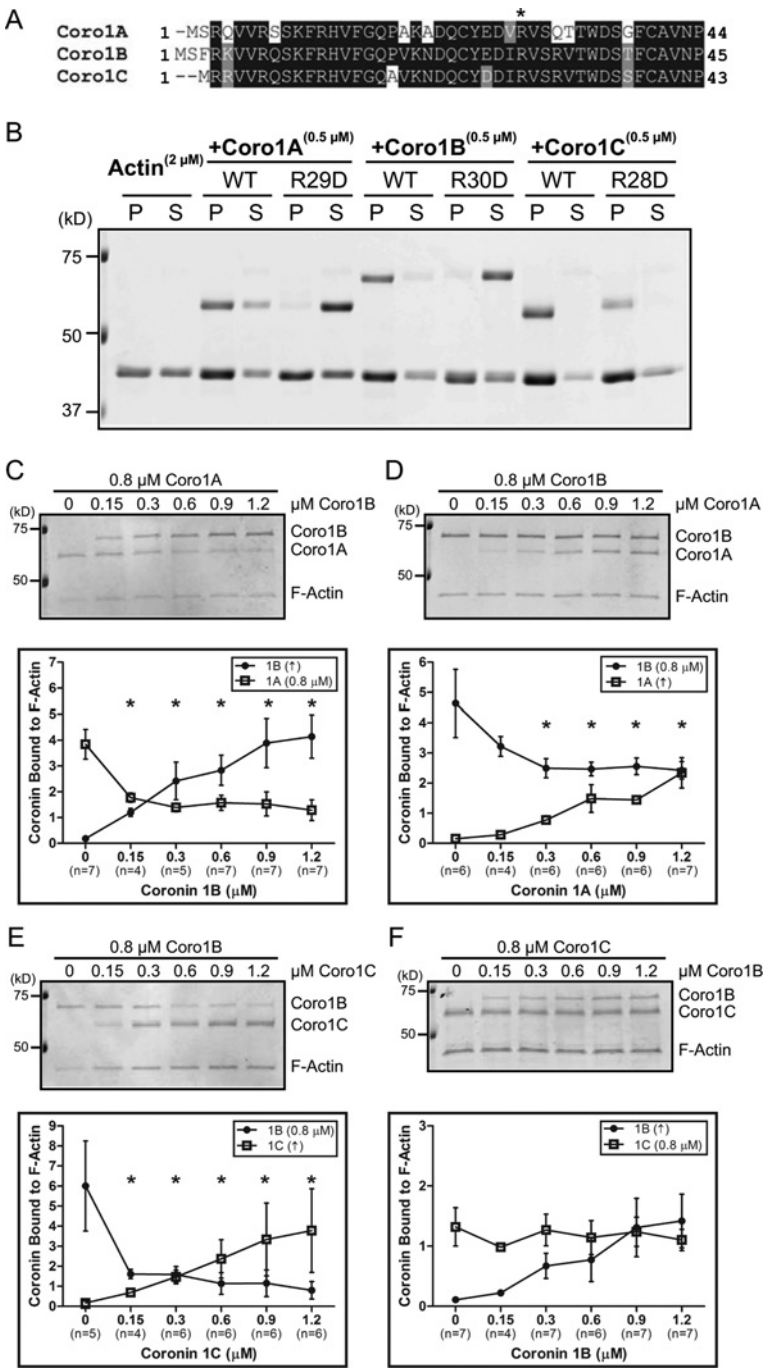

Figure 1 Mutation of a conserved arginine residue abolishes F-actin binding in Coro1A and Coro1B, but not Coro1C

(**A**) Protein sequence alignment of human Coro1 N-terminus. *Conserved arginine residue on the β-propeller shown previously to be involved in F-actin binding for Coro1B. (**B**) Actin cosedimentation was performed using 2 μM actin alone or with 0.5 μM Coro1A, Coro1B, Coro1C and their respective Arg→Asp mutants (R29D, R30D and R28D). Pellet (P) and supernatant (S) fractions were separated by SDS/PAGE. Representative Coomassie Blue-stained gel is from at least three independent experiments. Coro1A (**C**), Coro1B (**D** and **E**), or Coro1C (**F**) (0.8 μM) was incubated with 0.3 μM actin followed by incubation with increasing concentrations of the indicated coronin. Actin cosedimentation was performed and pellet fractions were separated by SDS/PAGE. Representative Coomassie Blue-stained gels are from at least four independent experiments. Quantification is shown as amount of coronin bound to F-actin, which was normalized to the amount of actin in the pellet. Results are means $\pm$ S.E.M. from the indicated number of experiments (n). Asterisk indicates statistical significance compared with initial concentration of coronin by one-way ANOVA; *$P < 0.05$. WT, wild-type. In all gels, molecular mass markers are shown in kDa on the left-hand side.

Coro1C unique region that was not present in other Coro1s. These residues were highly conserved amongst all vertebrate Coro1C orthologues (Figure 2A). To test whether the unique region is involved in F-actin binding, we mutated several of these conserved charged residues and performed actin cosedimentation assays using purified (full-length) mutant proteins (Figure 2B). Charge-reversal mutations in acidic residues (E379K, D431K and E438K) in combination with the R28D mutation did not affect Coro1C binding to F-actin. In addition, neither conservative alanine residue substitutions in a positive lysine patch [K418A, K419A/K427A and K428A (2×KA)] nor charge-reversal mutations [K418E, K419E/K427E and K428E (2×KE)] markedly

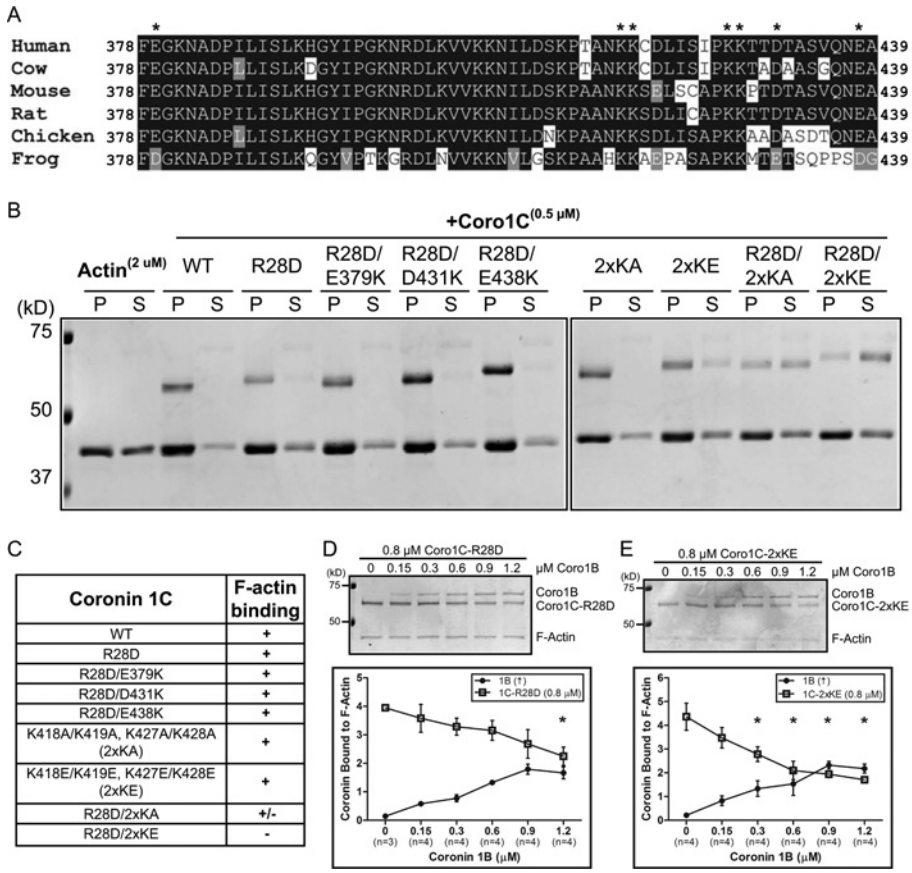

Coronin 1C	F-actin binding
WT	+
R28D	+
R28D/E379K	+
R28D/D431K	+
R28D/E438K	+
K418A/K419A, K427A/K428A (2xKA)	+
K418E/K419E, K427E/K428E (2xKE)	+
R28D/2xKA	+/-
R28D/2xKE	-

Figure 2 Coro1C harbours a second actin-binding site

(**A**) Protein sequence alignment of the vertebrate Coro1C unique region. *Charged residues mutated for assays in (**B**). (**B**) Actin cosedimentation was performed using 2 μM actin alone or with 0.5 μM wild-type (WT) Coro1C or the following mutants: R28D; R28D/E379K; R28D/D431K; R28D/E438K; K418A, K419A/K427A, K428A (2xKA); K418E, K419E/K427E, K428E (2×KE); R28D/2xKA; or R28D/2xKE. Pellet (P) and supernatant (S) fractions were separated by SDS/PAGE. Representative Coomassie Blue-stained gel is from at least three independent experiments. (**C**) Table summarizing actin cosedimentation results from (**B**). Coro1C–R28D (**D**) or Coro1C–2xKE (**E**) (0.8 μM) was incubated with 0.3 μM actin followed by incubation with increasing concentrations of Coro1B. Actin cosedimentation was performed and pellet fractions were separated by SDS/PAGE. Representative Coomassie Blue-stained gels are from four independent experiments. Quantification is shown as amount of coronin bound to F-actin, which was normalized to the amount of actin in the pellet. Results are means ± S.E.M. from the indicated number of experiments (*n*). Asterisk indicates statistical significance compared with initial concentration of coronin by one-way ANOVA; $^*P < 0.05$. In all gels, molecular mass markers are shown in kDa on the left-hand side.

affected F-actin binding. Interestingly, the R28D together with the 2×KA mutation reduced binding. Strikingly, only the 2×KE in conjunction with the R28D mutation abolished Coro1C binding to F-actin (summarized in Figure 2C). To further confirm these results, we repeated biochemical competition experiments using actin cosedimentation by pre-binding Coro1C–R28D (Figure 2D) or Coro1C–2×KE (Figure 2E) to actin filaments and adding increasing concentrations of Coro1B. Mutations at either of these sites allowed Coro1B to compete for binding to F-actin. Moreover, both Coro1C–R28D and Coro1C–2×KE were able to compete with Coro1B (Supplementary Figure S3 at http://www.BiochemJ.org/bj/444/bj4440089add.htm). Together, these data suggest that Coro1C has two sites that function collaboratively to promote binding to F-actin.

Coro1C binds F-actin co-operatively and with high affinity

We reasoned that the presence of two actin-binding sites should impart Coro1C with the ability to bind F-actin with higher affinity relative to other Coro1s. In the present study, we systematically compared Coro1 binding to preformed filaments from human platelet actin, which contains 85 % β-actin and 15 % γ-actin [32]. To calculate the binding affinity, we used a method to analyse the amount of coronin (0.1 μM input) depleted from the supernatant with increasing concentrations of actin in cosedimentation assays (Figure 3A). Among the Coro1s, Coro1A bound to platelet actin with the lowest affinity with $K_d = 2.569$ μM (Figure 3B), whereas Coro1B displayed a substantially higher affinity with a $K_d = 0.467$ μM (Figure 3C). Strikingly, in initial experiments using the same concentration of Coro1C, we observed rapid depletion even at concentrations just above the critical concentration of actin (results not shown), indicating that Coro1C binds F-actin with very high affinity. Therefore, to more accurately measure the affinity, we used a higher input concentration of Coro1C (0.3 μM). We consistently observed a steep depletion of Coro1C from the supernatant at concentrations of actin between 0.2–0.8 μM (Figures 3A and 3D), which was not apparent for either Coro1A or Coro1B.

We surmised that these effects might be due to co-operative effects of Coro1C binding to enhance the ability of additional Coro1C to bind F-actin. To further analyse this phenomenon, we attempted to fit binding curves to our experimental data using Hill slopes. Consistent with our hypothesis, Coro1A and Coro1B bound F-actin non-co-operatively with a Hill coefficient of ~1. In contrast, Coro1C showed a high degree of positive co-operativity with a Hill coefficient of 3.922. We also examined the effects of the R28D or 2×KE mutation on Coro1C binding affinity (Figures 3D and 3E). Intriguingly, although either mutation only modestly

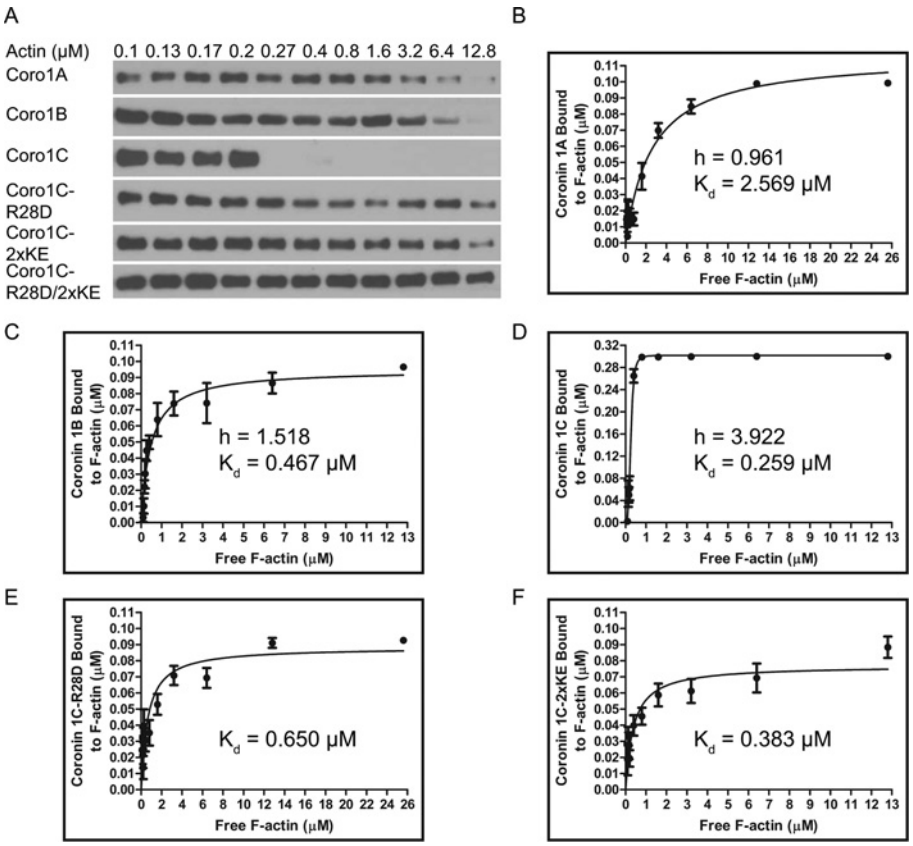

Figure 3 Coro1C binds F-actin co-operatively and with high affinity

(**A**) Coro1A, Coro1B, Coro1C–R28D, Coro1C–2×KE, Coro1C–R28D/2×KE (0.1 μM) or Coro1C (0.3 μM) was incubated with increasing concentrations of actin and cosedimentation assays were performed. Supernatant fractions were separated by SDS/PAGE and analysed by immunoblotting with an anti-His antibody. Representative immunoblots are from at least four independent experiments. Quantification of the amount of Coro1A (**B**), Coro1B (**C**), Coro1C (**D**), Coro1C–R28D (**E**) and Coro1C–2×KE (**F**) bound to F-actin as a function of the free F-actin concentration. Each data point is shown as mean ± S.E.M. from at least four independent experiments. Binding curves were fitted to the experimental data and used to generate a Hill coefficient (h) and dissociation constant (K_d), which are displayed on the plots.

impaired binding affinity, both were sufficient to block Coro1C-positive co-operative binding to F-actin (results not shown). In line with our actin cosedimentation data, mutation of both sites in combination severely decreased F-actin binding affinity ($\sim K_d > 25$ μM, results not shown). Overall, our data demonstrate that binding of Coro1C to F-actin requires both residues in the β-propeller and in the unique region. Furthermore, co-operative binding is a property that distinguishes Coro1C from other Coro1s.

Arg^{28} is the key determinant for efficient leading-edge localization of Coro1C, but both sites are required for actin binding *in vivo*

We previously demonstrated that efficient leading edge lamellipodia localization of Coro1B requires its F-actin-binding function [22]. The generation of an actin-binding-deficient mutant of Coro1C allowed us to address the specific effect of F-actin binding on its leading-edge localization *in vivo*. We first generated a monoclonal antibody that specifically recognized Coro1C, but not other coronins (Supplementary Figure S4 at http://www.BiochemJ.org/bj/444/bj4440089add.htm). We then simultaneously depleted endogenous Coro1C and re-expressed shRNA-resistant Coro1C–GFP and the R28D, 2×KE and R28D/2×KE mutants in IA32 mouse fibroblasts using a system we had developed previously (Figure 4A; [33]). The localization of wild-type and mutant Coro1C–GFP was examined in cells stained for cortactin (a leading-edge marker) and F-actin (Figure 4B). We analysed leading-edge localization of Coro1C using a contour-based method for determining the average fluorescence intensity of all the pixels along a contour edge (Figure 4C; [6]). We plotted the normalized cortactin and GFP fluorescence intensity as a function of the distance from the leading edge of the cell (Figure 4D). To quantify the amount of coronin at leading edge lamellipodia relative to the cytoplasm, we used a previously developed index of leading-edge enrichment [22]. This is defined as the ratio of the lamellipodia maximum intensity and the minimum cytoplasmic intensity (Figure 4E). As expected, Coro1C–GFP localized efficiently to the leading edge. In contrast, whereas the leading-edge enrichment of cortactin remained unchanged (results not shown), the localization of the actin-binding mutant Coro1C–GFP–R28D/2×KE was significantly impaired. The R28D mutation impaired leading edge enrichment of Coro1C almost to the same extent as the R28D/2×KE mutation, suggesting that whereas the R28D mutation failed to block actin binding *in vitro*, it was sufficient to impair leading-edge enrichment of Coro1C *in vivo*. Interestingly, the 2×KE mutant did not affect the leading-edge enrichment of Coro1C. These data demonstrate that, like Coro1B, efficient leading-edge localization of Coro1C requires the conserved site in the β-propeller.

Since the coronin at the leading edge lamellipodia represents only a subset of the total coronin in the cell, we further analysed

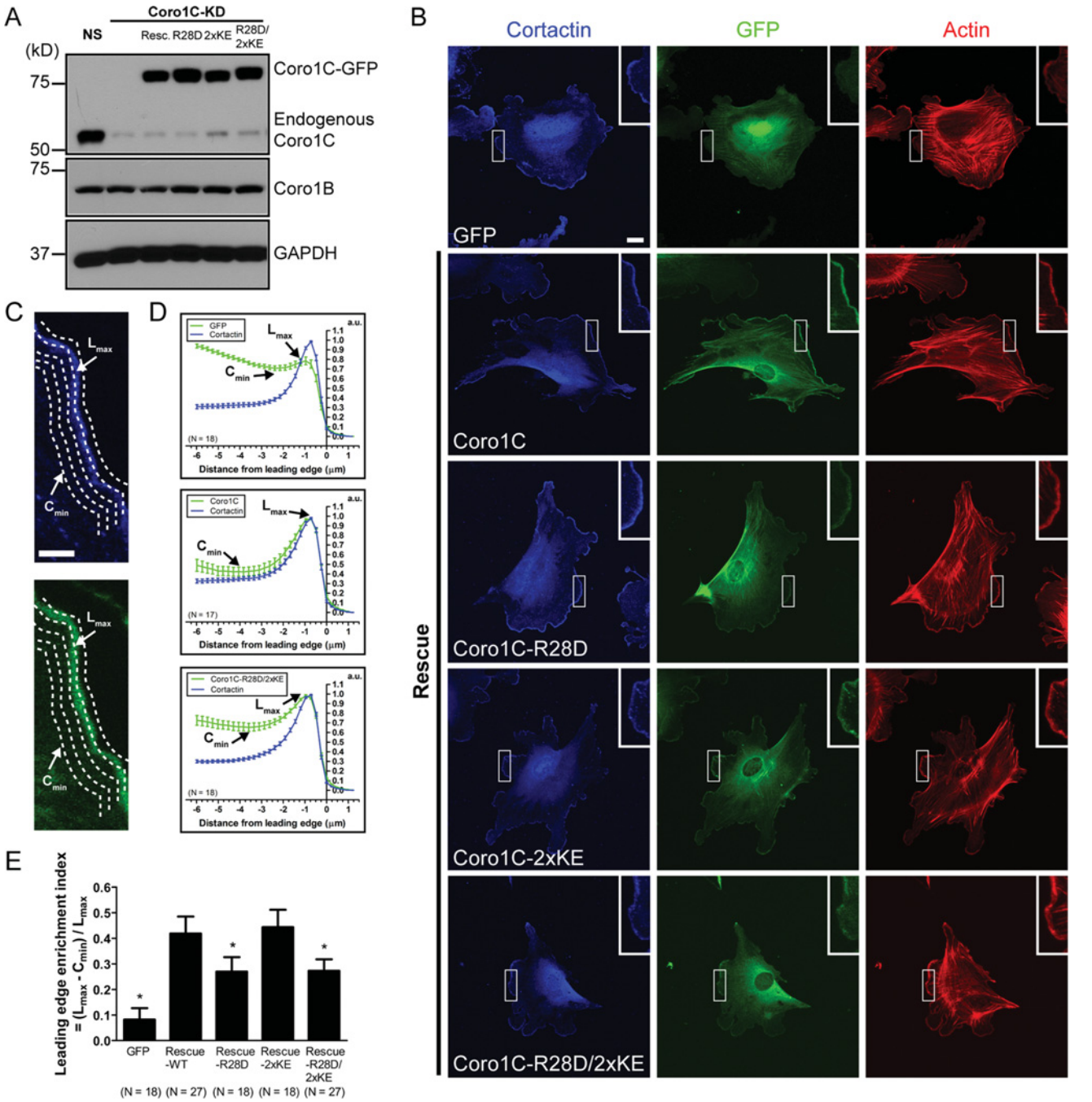

Figure 4 Arg[28] is the key determinant for efficient leading-edge localization of Coro1C, but both sites are required for actin binding *in vivo*

(**A**) IA32 mouse fibroblasts were infected with lentivirus expressing NS shRNA (GFP), Coro1C shRNA (Coro1C-KD) or Coro1C shRNA and re-expressing Coro1C–GFP (resc.) or R28D, 2×KE, R28D/2×KE mutants. Lysates were separated on SDS/PAGE and analysed by immunoblotting with anti-Coro1C and anti-Coro1B antibodies. GAPDH (glyceraldehyde-3-phosphate dehydrogenase) was probed as a loading control. (**B**) IA32 mouse fibroblasts expressing GFP or depleted of endogenous Coro1C and re-expressing (rescue) Coro1C–GFP, Coro1C–GFP–R28D, Coro1C–GFP–2×KE or Coro1C–GFP–R28D/2×KE were stained with an anti-cortactin antibody and phalloidin to label actin. Scale bar, 20 μm. Insets show magnified regions of the lamellipodia. (**C**) Magnified region of the lamellipodia in IA32 mouse fibroblasts re-expressing Coro1C–GFP depicts an example schematic of leading edge contour analysis. Scale bar, 5 μm. The average fluorescence intensity of cortactin and GFP for all the pixels along a contour edge was measured. L_{max} is the maximum fluorescence intensity in the lamellipodia. C_{min} is the minimum fluorescence intensity in the cytoplasm. (**D**) Fluorescence intensities from contour edge analysis were normalized. Representative plots were generated from normalized fluorescence intensities as a function of distance from the leading edge for cortactin and GFP combined from indicated number of cells (N). Results are means ± S.E.M. a.u., absorbance units. (**E**) Quantification of relative leading-edge enrichment index from indicated number of cells (N), which is defined as $(L_{max} - C_{min})/L_{max}$. $^*P < 0.01$ compared with wild-type Coro1C–GFP rescue by one-way ANOVA with Dunnett post-test. Results are means ± 95 % confidence interval.

the global Coro1C distribution by separating cell lysates into supernatant and Triton-insoluble fractions (Supplementary Figure S5 at http://www.BiochemJ.org/bj/444/bj4440089add.htm). As anticipated, wild-type Coro1C–GFP was associated with the Triton-insoluble cytoskeletal fraction. Coro1C–R28D and Coro1C–2×KE were also found in the Triton-insoluble compartment. Interestingly, a greater amount of the R28D mutant was present in the supernatant. In line with our actin

cosedimentation data, the fully defective R28D/2×KE actin-binding mutant was exclusively detected in the supernatant. Together, these data suggest that, although the conserved arginine residue in the β-propeller is a key determinant in leading-edge localization, both sites in the β-propeller and the unique region of Coro1C are required for global association with the actin cytoskeleton *in vivo*.

DISCUSSION

On the basis of our findings, we provide additional insight into the F-actin-binding function of the mammalian Coro1s. We have substantial evidence to support the idea that Coro1C harbours a second actin-binding site. First, a mutation in a conserved arginine residue in Coro1A and Coro1B that abrogated F-actin binding did not block F-actin binding in Coro1C. Secondly, charge-reversal mutations in the positive patch in the unique region blocked F-actin binding only when in combination with the R28D mutation. Thirdly, the F-actin-binding affinity of Coro1C with either of these mutations was not dramatically affected. Moreover, we demonstrated that an actin-binding mutant of Coro1C was not enriched in leading-edge lamellipodia in fibroblasts, reinforcing the general notion that F-actin binding is essential for coronin function.

One initial interpretation of our coronin competition results was that they might only reflect differences in actin-binding affinity. However, our measurements of the binding affinities suggest that this is not the case. Coro1A has a substantially lower affinity for F-actin than Coro1B, but it was able to compete with Coro1B for binding. On the other hand, Coro1B and Coro1C share similar binding affinities, but Coro1B was unable to compete with Coro1C. It is possible that inability of Coro1B to compete with Coro1C may also be related to the ability of Coro1C to bind F-actin co-operatively. Mutations in the site in β-propeller or in the unique region had only modest effects on Coro1C-binding affinity, but allowed Coro1B to compete for binding to actin, suggesting that the location of the these binding sites may be in close proximity on the actin filament.

To validate our *in vitro* results, we examined the localization of Coro1C and found that actin binding is required for efficient leading-edge localization. However, one distinction from our *in vitro* results is that the R28D mutation was sufficient to block leading-edge localization *in vivo*, whereas the 2×KE mutant Coro1C still retained leading edge localization. This raises the possibility that the conserved site in the β-propeller has a function in addition to its role in actin binding. Indeed, a previous study demonstrated that mutation of this site in Coro1A abolished phospholipid binding [30]. Alternatively, either the 2×KE mutation impairs Coro1C localization to other actin-based structures or alters a behaviour not evident in our leading-edge localization studies. Indeed, we confirmed this effect by finding that the R28D/2×KE mutant was completely excluded from the Triton-insoluble cytoskeleton. In the future it will be interesting to distinguish between the differential effects of both actin-binding sites on Coro1C localization and function.

By performing binding affinity measurements, we were able to determine that a unique function for Coro1C is that it displays highly co-operative binding to actin filaments. There are only a few other known examples of modulators that bind actin co-operatively: cofilin, tropomyosin, gelsolin and myosin subfragment-1 [34–37]. Intriguingly, cofilin co-operative binding has been postulated to propagate structural changes along the filament to lower the affinity of actin for the Arp2/3 complex [38]. At present, we cannot discern if Coro1C co-operativity is due to Coro1C–Coro1C interactions or the ability of Coro1C to alter the structure of the actin filament to enhance the affinity for additional Coro1C. It is tempting to speculate that these effects may be related to the nucleotide state of actin, as our previous results suggest that Coro1B binds preferentially to ATP- and ADP-P_i-actin over ADP-actin with approximately 50-fold higher affinity [22].

Coronins facilitate actin dynamics at the level of Arp2/3 actin assembly and cofilin-mediated disassembly. Both Coro1A and Coro1B contain a phosphorylation site by PKC (protein kinase C) at Ser^2 which regulates the interaction of Coro1A and Coro1B with the Arp2/3 complex and has effects on whole-cell motility [4, 5]. Intriguingly, Coro1C lacks this phosphorylation site and can still interact with the Arp2/3 complex [8], which may contribute to the residual localization observed with the Coro1C actin-binding mutant. In contrast with a previous study suggesting that Coro1A and cofilin synergize to promote actin depolymerization [39], Coro1A and Coro1B protect actin filaments from cofilin binding. Instead, Coro1B targets the cofilin-activating phosphatase Slingshot-1 to the leading edge of migrating cells, suggesting a more indirect mechanism by which coronins facilitate cofilin activity [6]. It will be interesting to determine how Coro1C co-operative binding affects these processes.

With the generation of a completely deficient actin-binding mutant of Coro1C, we now have the ability to formally assess the actin-binding function of Coro1C in a variety of physiological contexts. A future challenge will be to determine the biophysical properties of Coro1C co-operative binding and how this feature mechanistically contributes to the regulation of actin cytoskeletal dynamics.

AUTHOR CONTRIBUTION

Keefe Chan performed the experiments. David Roadcap and Nicholas Holoweckyj generated and tested the Coro1C monoclonal antibody. Keefe Chan and James Bear designed the experiments, analysed the data and wrote the paper.

ACKNOWLEDGEMENTS

We thank Tao Bo for technical assistance and members of the Bear lab for helpful discussions.

FUNDING

This work was supported by the National Institutes of Health [grant number G-M083-35], the American Chemical Society [grant number RSG-08-157-01], and the Howard Hughes Medical Institute.

REFERENCES

1 de Hostos, E. L., Bradtke, B., Lottspeich, F., Guggenheim, R. and Gerisch, G. (1991) Coronin, an actin binding protein of *Dictyostelium discoideum* localized to cell surface projections, has sequence similarities to G-protein β subunits. EMBO J. **10**, 4097–4104
2 Chan, K. T., Creed, S. J. and Bear, J. E. (2011) Unraveling the enigma: progress towards understanding the coronin family of actin regulators. Trends Cell Biol. **21**, 481–488
3 Uetrecht, A. C. and Bear, J. E. (2006) Coronins: the return of the crown. Trends Cell Biol. **16**, 421–426
4 Foger, N., Rangell, L., Danilenko, D. M. and Chan, A. C. (2006) Requirement for coronin 1 in T lymphocyte trafficking and cellular homeostasis. Science **313**, 839–842
5 Cai, L., Holoweckyj, N., Schaller, M. D. and Bear, J. E. (2005) Phosphorylation of coronin 1B by protein kinase C regulates interaction with Arp2/3 and cell motility. J. Biol. Chem. **280**, 31913–31923
6 Cai, L., Marshall, T. W., Uetrecht, A. C., Schafer, D. A. and Bear, J. E. (2007) Coronin 1B coordinates Arp2/3 complex and cofilin activities at the leading edge. Cell **128**, 915–929
7 Iizaka, M., Han, H. J., Akashi, H., Furukawa, Y., Nakajima, Y., Sugano, S., Ogawa, M. and Nakamura, Y. (2000) Isolation and chromosomal assignment of a novel human gene, *CORO1C*, homologous to coronin-like actin-binding proteins. Cytogenet. Cell Genet. **88**, 221–224
8 Rosentreter, A., Hofmann, A., Xavier, C. P., Stumpf, M., Noegel, A. A. and Clemen, C. S. (2007) Coronin 3 involvement in F-actin-dependent processes at the cell cortex. Exp. Cell Res. **313**, 878–895

9 Spoerl, Z., Stumpf, M., Noegel, A. A. and Hasse, A. (2002) Oligomerization, F-actin interaction, and membrane association of the ubiquitous mammalian coronin 3 are mediated by its carboxyl terminus. J. Biol. Chem. **277**, 48858–48867

10 Kimura, T., Kaneko, Y., Yamada, S., Ishihara, H., Senda, T., Iwamatsu, A. and Niki, I. (2008) The GDP-dependent Rab27a effector coronin 3 controls endocytosis of secretory membrane in insulin-secreting cell lines. J. Cell Sci. **121**, 3092–3098

11 Thal, D., Xavier, C. P., Rosentreter, A., Linder, S., Friedrichs, B., Waha, A., Pietsch, T., Stumpf, M., Noegel, A. and Clemen, C. (2008) Expression of coronin-3 (coronin-1C) in diffuse gliomas is related to malignancy. J. Pathol. **214**, 415–424

12 Appleton, B. A., Wu, P. and Wiesmann, C. (2006) The crystal structure of murine coronin-1: a regulator of actin cytoskeletal dynamics in lymphocytes. Structure **14**, 87–96

13 Stirnimann, C. U., Petsalaki, E., Russell, R. B. and Muller, C. W. (2010) WD40 proteins propel cellular networks. Trends Biochem. Sci. **35**, 565–574

14 Goode, B. L., Wong, J. J., Butty, A. C., Peter, M., McCormack, A. L., Yates, J. R., Drubin, D. G. and Barnes, G. (1999) Coronin promotes the rapid assembly and cross-linking of actin filaments and may link the actin and microtubule cytoskeletons in yeast. J. Cell Biol. **144**, 83–98

15 Liu, S. L., Needham, K. M., May, J. R. and Nolen, B. J. (2011) Mechanism of a concentration-dependent switch between activation and inhibition of Arp2/3 complex by coronin. J. Biol. Chem. **286**, 17039–17046

16 Oku, T., Itoh, S., Ishii, R., Suzuki, K., Nauseef, W. M., Toyoshima, S. and Tsuji, T. (2005) Homotypic dimerization of the actin-binding protein p57/coronin-1 mediated by a leucine zipper motif in the C-terminal region. Biochem. J. **387**, 325–331

17 Kammerer, R. A., Kostrewa, D., Progias, P., Honnappa, S., Avila, D., Lustig, A., Winkler, F. K., Pieters, J. and Steinmetz, M. O. (2005) A conserved trimerization motif controls the topology of short coiled coils. Proc. Natl. Acad. Sci. U.S.A. **102**, 13891–13896

18 Gatfield, J., Albrecht, I., Zanolari, B., Steinmetz, M. O. and Pieters, J. (2005) Association of the leukocyte plasma membrane with the actin cytoskeleton through coiled coil-mediated trimeric coronin 1 molecules. Mol. Biol. Cell **16**, 2786–2798

19 Liu, C. Z., Chen, Y. and Sui, S. F. (2006) The identification of a new actin-binding region in p57. Cell Res. **16**, 106–112

20 Oku, T., Itoh, S., Okano, M., Suzuki, A., Suzuki, K., Nakajin, S., Tsuji, T., Nauseef, W. M. and Toyoshima, S. (2003) Two regions responsible for the actin binding of p57, a mammalian coronin family actin-binding protein. Biol. Pharm. Bull. **26**, 409–416

21 Mishima, M. and Nishida, E. (1999) Coronin localizes to leading edges and is involved in cell spreading and lamellipodium extension in vertebrate cells. J. Cell Sci. **112**, 2833–2842

22 Cai, L., Makhov, A. M. and Bear, J. E. (2007) F-actin binding is essential for coronin 1B function *in vivo*. J. Cell Sci. **120**, 1779–1790

23 Galkin, V. E., Orlova, A., Brieher, W., Kueh, H. Y., Mitchison, T. J. and Egelman, E. H. (2008) Coronin-1A stabilizes F-actin by bridging adjacent actin protomers and stapling opposite strands of the actin filament. J. Mol. Biol. **376**, 607–613

24 Gandhi, M., Jangi, M. and Goode, B. L. (2010) Functional surfaces on the actin-binding protein coronin revealed by systematic mutagenesis. J. Biol. Chem. **285**, 34899–34908

25 Gandhi, M., Achard, V., Blanchoin, L. and Goode, B. L. (2009) Coronin switches roles in actin disassembly depending on the nucleotide state of actin. Mol. Cell **34**, 364–374

26 Cai, L., Makhov, A. M., Schafer, D. A. and Bear, J. E. (2008) Coronin 1B antagonizes cortactin and remodels Arp2/3-containing actin branches in lamellipodia. Cell **134**, 828–842

27 Rubinson, D. A., Dillon, C. P., Kwiatkowski, A. V., Sievers, C., Yang, L., Kopinja, J., Rooney, D. L., Zhang, M., Ihrig, M. M., McManus, M. T. et al. (2003) A lentivirus-based system to functionally silence genes in primary mammalian cells, stem cells and transgenic mice by RNA interference. Nat. Genet. **33**, 401–406

28 Bryce, N. S., Clark, E. S., Leysath, J. L., Currie, J. D., Webb, D. J. and Weaver, A. M. (2005) Cortactin promotes cell motility by enhancing lamellipodial persistence. Curr. Biol. **15**, 1276–1285

29 Bear, J. E., Loureiro, J. J., Libova, I., Fassler, R., Wehland, J. and Gertler, F. B. (2000) Negative regulation of fibroblast motility by Ena/VASP proteins. Cell **101**, 717–728

30 Tsujita, K., Itoh, T., Kondo, A., Oyama, M., Kozuka-Hata, H., Irino, Y., Hasegawa, J. and Takenawa, T. (2010) Proteome of acidic phospholipid-binding proteins: spatial and temporal regulation of Coronin 1A by phosphoinositides. J. Biol. Chem. **285**, 6781–6789

31 Foger, N., Jenckel, A., Orinska, Z., Lee, K. H., Chan, A. C. and Bulfone-Paus, S. (2011) Differential regulation of mast cell degranulation versus cytokine secretion by the actin regulatory proteins Coronin1a and Coronin1b. J. Exp. Med. **208**, 1777–1787

32 De La Cruz, E. M. (2005) Cofilin binding to muscle and non-muscle actin filaments: isoform-dependent cooperative interactions. J. Mol. Biol. **346**, 557–564

33 Vitriol, E. A., Uetrecht, A. C., Shen, F., Jacobson, K. and Bear, J. E. (2007) Enhanced EGFP-chromophore-assisted laser inactivation using deficient cells rescued with functional EGFP-fusion proteins. Proc. Natl. Acad. Sci. U.S.A. **104**, 6702–6707

34 McGough, A., Pope, B., Chiu, W. and Weeds, A. (1997) Cofilin changes the twist of F-actin: implications for actin filament dynamics and cellular function. J. Cell Biol. **138**, 771–781

35 Yang, Y. Z., Korn, E. D. and Eisenberg, E. (1979) Cooperative binding of tropomyosin to muscle and *Acanthamoeba* actin. J. Biol. Chem. **254**, 7137–7140

36 Prochniewicz, E., Zhang, Q., Janmey, P. A. and Thomas, D. D. (1996) Cooperativity in F-actin: binding of gelsolin at the barbed end affects structure and dynamics of the whole filament. J. Mol. Biol. **260**, 756–766

37 Greene, L. E. and Eisenberg, E. (1980) Cooperative binding of myosin subfragment-1 to the actin–troponin–tropomyosin complex. Proc. Natl. Acad. Sci. U.S.A. **77**, 2616–2620

38 Chan, C., Beltzner, C. C. and Pollard, T. D. (2009) Cofilin dissociates Arp2/3 complex and branches from actin filaments. Curr. Biol. **19**, 537–545

39 Brieher, W. M., Kueh, H. Y., Ballif, B. A. and Mitchison, T. J. (2006) Rapid actin monomer-insensitive depolymerization of *Listeria* actin comet tails by cofilin, coronin, and Aip1. J. Cell Biol. **175**, 315–324

Received 2 February 2012/23 February 2012; accepted 27 February 2012
Published as BJ Immediate Publication 27 February 2012, doi:10.1042/BJ20120209

Biochem. J. (2012) **444**, 89–96 (Printed in Great Britain) doi:10.1042/BJ20120209

online data

SUPPLEMENTARY ONLINE DATA

Coronin 1C harbours a second actin-binding site that confers co-operative binding to F-actin

Keefe T. CHAN*†, David W. ROADCAP*, Nicholas HOLOWECKYJ* and James E. BEAR*†[1]

*Lineberger Comprehensive Cancer Center and Department of Cellular and Developmental Biology, University of North Carolina at Chapel Hill, NC 27599, U.S.A., and †Howard Hughes Medical Institute, University of North Carolina at Chapel Hill, NC 27599, U.S.A.

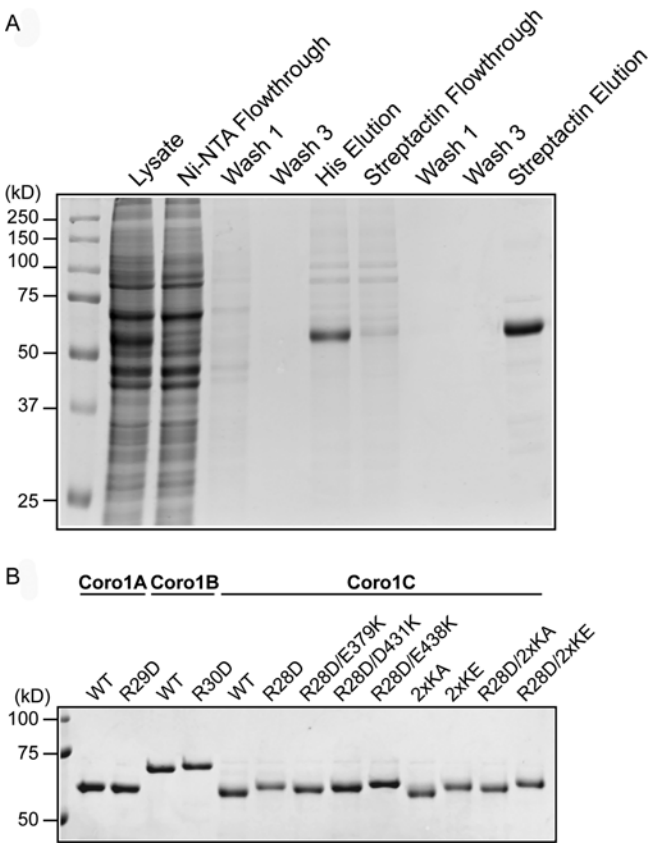

Figure S1 Purification of mammalian Coro1 proteins

(**A**) Coomassie Blue-stained gel shows purification steps for recombinant Coro1C, which contains a C-terminal Strep–His_8 tag. (**B**) Purified wild-type (WT) and mutant coronin proteins (0.5 μg) used for *in vitro* studies were separated by SDS/PAGE and subjected to Coomassie Blue staining. Molecular masses are shown in kDa on the left-hand side. Ni-NTA, Ni^{2+}-nitrilotriacetate.

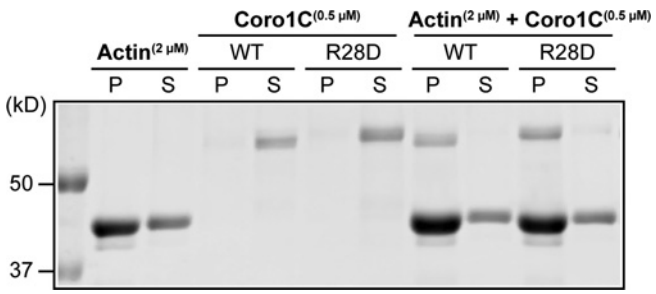

Figure S2 Actin cosedimentation control for Coro1C and Coro1C–R28D

Cosedimentation assays were performed using 0.5 μM Coro1C or Coro1C–R28D with and without 2 μM actin. Pellet (P) and supernatant (S) fractions were analysed by SDS/PAGE and subjected to Coomassie Blue staining. Molecular masses are shown in kDa on the left-hand side. WT, wild-type.

[1] To whom correspondence should be addressed (email jbear@email.unc.edu).

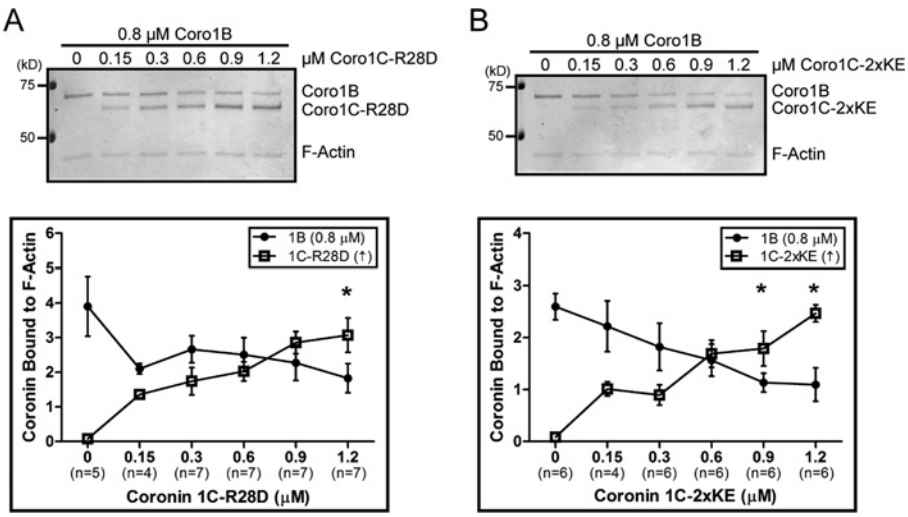

Figure S3 Coro1B competes with Coro1C–R28D and Coro1C–2×KE for binding to F-actin

Coro1B (0.8 μM) was incubated with actin (0.3 μM) for 1 h followed by incubation with increasing concentrations of Coro1C–R28D (**A**) or Coro1C–2×KE (**B**). Actin cosedimentation was performed and pellet fractions were subjected to SDS/PAGE and Coomassie Blue staining. Quantification of the relative amount of Coronin bound to F-actin from the indicated number of independent experiments (*n*) is shown as means ± S.E.M. $^*P < 0.05$ determined by one-way ANOVA as compared with the initial concentration of coronin. Molecular masses are shown in kDa on the left-hand side of the gels.

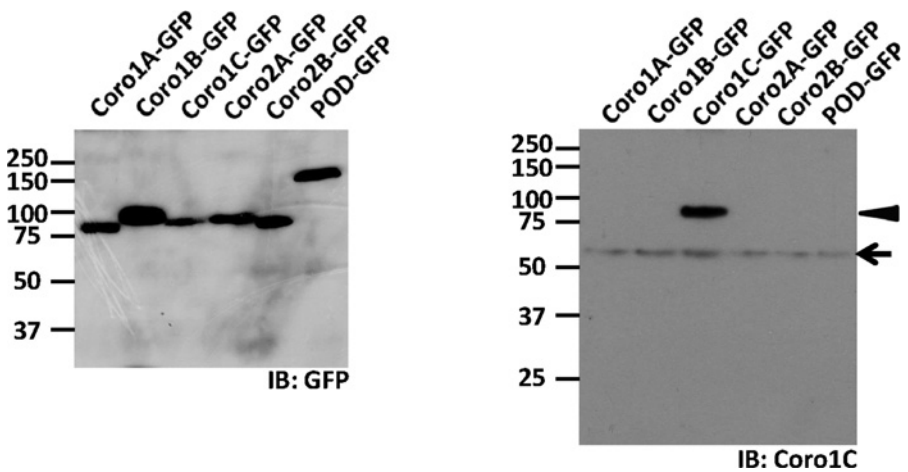

Figure S4 Specificity of anti-Coro1C antibody

(**A**) Lysates of HEK (human embryonic kidney)-293FT cells expressing GFP fusions of Coro1A, Coro1B, Coro1C, Coro2A, Coro2B or POD (polarity-osmotic defective) were separated by SDS/PAGE and analysed by immunoblotting (IB) with anti-GFP or anti-Coro1C antibodies. Arrow indicates endogenous Coro1C and arrowhead denotes Coro1C–GFP. Molecular masses are shown in kDa on the left-hand side.

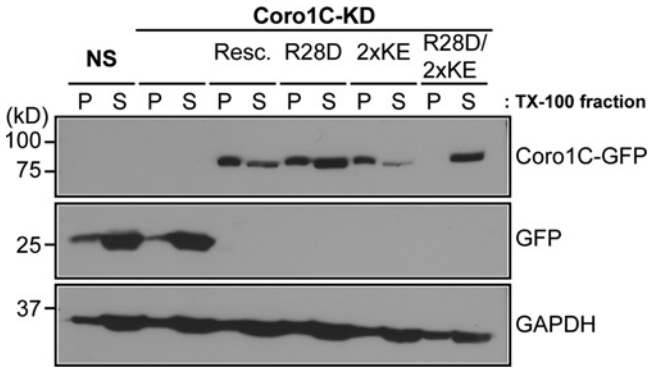

Figure S5 Analysis of Coro1C association with the detergent-insoluble cytoskeleton

IA32 mouse fibroblasts were infected with lentivirus expressing NS shRNA (GFP), Coro1C shRNA (Coro1C-KD) or Coro1C shRNA and re-expressing Coro1C–GFP (resc.) or R28D, 2×KE, R28D/2×KE mutants. Cells were lysed in RIPA buffer containing 1% Triton X-100 (TX-100) and subjected to centrifugation at 14000 ***g*** for 10 min. Detergent-insoluble pellets (P) and supernatants (S) were separated by SDS/PAGE and analysed by immunoblotting with an anti-GFP antibody. GAPDH (glyceraldehyde-3-phosphate dehydrogenase) was probed as a loading control. Molecular masses are shown in kDa on the left-hand side.

Received 2 February 2012/23 February 2012; accepted 27 February 2012
Published as BJ Immediate Publication 27 February 2012, doi:10.1042/BJ20120209